HHS Public Access

Author manuscript

*Circ Arrhythm Electrophysiol*. Author manuscript; available in PMC 2018 October 01.

Published in final edited form as:

*Circ Arrhythm Electrophysiol*. 2017 October ; 10(10): . doi:10.1161/CIRCEP.117.005267.

# Action Potential Shortening and Impairment of Cardiac Function by Ablation of *Slc26a6*

**Padmini Sirish, PhD**[1], **Hannah A. Ledford, BA**[1], **Valeriy Timofeyev, PhD**[1], **Phung N. Thai, PhD**[1], **Lu Ren, MD**[1], **Hyo Jeong Kim, PhD**[2,*], **Seojin Park, PhD**[1], **Jeong Han Lee, PhD**[3], **Gu Dai, PhD**[1], **Maryam Moshref, MS**[1], **Choong-Ryoul Sihn, PhD**[1], **Wei Chun Chen, PhD**[1], **Maria Valeryevna Timofeyeva, MS**[1,5], **Zhong Jian, PhD**[4], **Rafael Shimkunas, MS**[4,6], **Leighton T. Izu, PhD**[4], **Nipavan Chiamvimonvat, MD**[1,5], **Ye Chen-Izu, PhD**[1,4,6], **Ebenezer N. Yamoah, PhD**[3], and **Xiao-Dong Zhang, PhD**[1,5]

[1]Division of Cardiovascular Medicine, Department of Internal Medicine, University of California, Davis, CA

[2]Center for Neuroscience, University of California, Davis, CA

[3]Department of Physiology and Cell Biology, School of Medicine, University of Nevada, Reno, NV

[4]Department of Pharmacology, University of California, Davis, CA

[5]Department of Veterans Affairs, Northern California Health Care System, Mather, CA

[6]Department of Biomedical Engineering, University of California, Davis, CA

## Abstract

**Background—**Intracellular pH ($pH_i$) is critical to cardiac excitation and contraction; uncompensated changes in $pH_i$ impair cardiac function and trigger arrhythmia. Several ion transporters participate in cardiac $pH_i$ regulation. Our previous studies identified several isoforms of a solute carrier Slc26a6 to be highly expressed in cardiomyocytes. We show that Slc26a6 mediates electrogenic $Cl^-/HCO_3^-$ exchange activities in cardiomyocytes, suggesting the potential role of Slc26a6 in regulation of not only $pH_i$, but also cardiac excitability.

**Methods and Results—**To test the mechanistic role of Slc26a6 in the heart, we took advantage of *Slc26a6* knockout (*Slc26a6*$^{-/-}$) mice using both *in vivo* and *in vitro* analyses. Consistent with our prediction of its electrogenic activities, ablation of *Slc26a6* results in action potential (AP) shortening. There are reduced $Ca^{2+}$ transient and sarcoplasmic reticulum $Ca^{2+}$ load, together with decreased sarcomere shortening in *Slc26a6*$^{-/-}$ cardiomyocytes. These abnormalities translate into reduced fractional shortening and cardiac contractility at the *in vivo* level. Additionally, $pH_i$ is elevated in *Slc26a6*$^{-/-}$ cardiomyocytes with slower recovery kinetics from intracellular alkalization, consistent with the $Cl^-/HCO_3^-$ exchange activities of Slc26a6. Moreover, *Slc26a6*$^{-/-}$

Correspondence: Xiao-Dong Zhang, Ph.D., Division of Cardiovascular Medicine, Department of Internal Medicine, University of California, Davis, One Shields Avenue, GBSF 6303, Davis, CA 95616, Tel: (530) 752-9717, Fax: (530) 754-7167, xdzhang@ucdavis.edu.

*deceased

**Disclosures:** None.

mice show evidence of sinus bradycardia and fragmented QRS complex, supporting the critical role of Slc26a6 in cardiac conduction system.

**Conclusions—**Our study provides mechanistic insights into Slc26a6, a unique cardiac electrogenic $Cl^-/HCO_3^-$ transporter in ventricular myocytes, linking the critical roles of Slc26a6 in regulation of $pH_i$, excitability, and contractility. $pH_i$ is a critical regulator of other membrane and contractile proteins. Future studies are needed to investigate possible changes in these proteins in *Slc26a6*$^{-/-}$ mice.

### Keywords

Solute carrier; Slc26a6; action potential; cardiac function

### Journal Subject Terms

Ion channels/Membrane Transport; Electrophysiology; Arrhythmias; Basic Science Research; Contractile Function; Hemodynamics; Ischemia; Physiology

## Introduction

Acid-base balance is critical for maintaining normal cardiac function. An uncompensated shift of intracellular pH ($pH_i$) generates abnormal electrical activities, contractile disorder, and altered intracellular $Ca^{2+}$ signaling.[1, 2] The bicarbonate ($HCO_3^-$) / carbon dioxide ($CO_2$) buffering system plays a central role in regulation of $pH_i$. Therefore, transport of $HCO_3^-$ across the plasma membrane is critical in maintaining cellular pH homeostasis. Several $HCO_3^-$ transporters have been identified in cardiomyocytes, including $Na^+/HCO_3^-$ (NBC) co-transporter and $Cl^-/HCO_3^-$ exchanger (AE or CBE).[1] NBC mediates acid extrusion, while AE mediates acid loading.

Solute carrier Slc26a6 is a versatile anion exchanger, first identified in epithelial cells, with abundant expression in kidneys, pancreas, intestines, and placenta.[3–5] It mediates $Cl^-$/oxalate, $Cl^-/HCO_3^-$, $Cl^-/OH^-$, $Cl^-/SO_4^{2-}$, and $Cl^-$/formate exchange activities. It was previously reported that Slc26a6 is the predominant $Cl^-/HCO_3^-$ and $Cl^-/OH^-$ exchanger in the mouse heart, based on the transcript levels.[6] Our recent functional study identified four cardiac Slc26a6 isoforms, which mediate $Cl^-/HCO_3^-$ exchange in atrial and ventricular myocytes[7]. Importantly, we found that $Cl^-/HCO_3^-$ exchange by cardiac Slc26a6 is electrogenic. Indeed, cardiac Slc26a6 represents the first electrogenic exchanger with only anionic substrates and provides active transport of $Cl^-$ into the cells to regulate intracellular $Cl^-$ homeostasis. In addition, activities of Slc26a6 are predicted to alter the $pH_i$ by transporting $HCO_3^-$ or $OH^-$. Therefore, we hypothesize that cardiac Slc26a6 may play a unique role in the regulation of not only $pH_i$, but also cardiac excitability and function.

To directly test the hypothesis, we took advantage of a *Slc26a6* knockout (*Slc26a6*$^{-/-}$) mouse model[8] using *in vivo* and *in vitro* analyses. Under physiological conditions, Slc26a6 activities are predicted to coincide with the dynamic range of cardiac action potential (AP), generating mainly inward currents, with outward current beyond ~ +36 mV[7]. Indeed, our study reveals that ablation of *Slc26a6* results in AP shortening, consistent with electrogenic

activities of Slc26a6. The shortened AP durations (APDs) result in reduced $Ca^{2+}$ transient and sarcoplasmic reticulum (SR) $Ca^{2+}$ load, along with decreased sarcomere shortening in *Slc26a6*$^{-/-}$ cardiomyocytes. These abnormalities translate into reduced fractional shortening and cardiac contractility at the *in vivo* level. Importantly, $pH_i$ is elevated in *Slc26a6*$^{-/-}$ cardiomyocytes with slower recovery kinetics from intracellular alkalization, consistent with $Cl^-/HCO_3^-$ exchange activities of Slc26a6. Moreover, *Slc26a6*$^{-/-}$ mice show evidence of sinus bradycardia and fragmented QRS complex, supporting the critical role of Slc26a6 in cardiac conduction system.

## Materials and Methods

All animal care and procedures were performed in accordance with the protocols approved by Institutional Animal Care and Use Committee of the University of California, Davis and in accordance with National Institutes of Health guidelines. De-identified human ventricular specimens were obtained from a commercial source, in accordance with the approved UC Davis Institutional Review Board (IRB) protocol. Please refer to the Online Supplemental Data for additional details.

We used 129S6/SvEv wild type (WT) and *Slc26a6*$^{-/-}$ mice previously generated and reported[8] (a generous gift from Dr. Peter S. Aronson, Yale University) in our study. All experiments described in the study were conducted in a blinded fashion.

### Cardiac tissue preparation and cardiomyocyte isolation

Mice were anesthetized by intraperitoneal injection of 80 mg/kg of ketamine and 5 mg/kg of xylazine. Cardiomyocytes were isolated as previously described[7]

### Genotyping, western blot, and histological analyses

Histological and western blot analyses of cardiac tissue were performed as we have previously described[9]. Genotyping analyses of *Slc26a6*$^{-/-}$ mice are presented in Supplemental Figure 1.

### Electrocardiographic Recordings

ECG recordings were performed as previously described[10, 11].

### Analysis of cardiac function by echocardiography

Echocardiograms to assess systolic function were performed in conscious animals as we have previously described.[10]

### Hemodynamic monitoring

Mice were anesthetized by intraperitoneal injection of 80 mg/kg of ketamine and 5 mg/kg of xylazine and maintained at 37 ºC. Recording of pressure and volume was performed by using Millar Pressure-Volume System MPVS-300 (Millar, Inc., Houston, TX), Power Lab, and Lab Chart 6.0 software (AD Instruments, Colorado Springs, CO).

### Patch-clamp recordings

Whole-cell current[7] and AP recordings[10] were performed as we have previously described. For current recordings, the clamped and suspended whole-cell was alternately exposed to two capillary tubes dispensing control and test solutions at a potential of 0 mV.[7] For the outward current recording, we used the same solutions as we previously documented[7].

For the inward current recording, the pipette solution contained (in mM): 24 $NaHCO_3$, 116 Na Glutamate, 1 EGTA, 1.4 NaCl, and gassed with 5% $CO_2$ and 95% $O_2$. The bath control solution was the same as pipette solution. The bath test solution with 140 mM $Cl^-$ contained (in mM): 140 NaCl, 10 HEPEs, 1 EGTA, and pH 7.4; the bath test solution with 14 mM $Cl^-$ contained (in mM): 14 NaCl, 126 Na Glutamate, 10 HEPEs, 1 EGTA, and pH 7.4. Current recordings were performed at the room temperature and APs were recorded at 36 °C.

### Measurement of sarcomere shortening and $Ca^{2+}$ transient (CaT)

We used IonOptix sarcomere detection (IonOptix LLC., Westwood, MA) and the fast Fourier transform (FFT) method[12]. Contraction was measured using a high-speed camera (MyoCam-S, 240 to 1000 frames/s) to record sarcomere movement. The sarcomere pattern was used to calculate the sarcomere length using an FFT algorithm. The fractional shortening was calculated as the percentage change in sarcomere length during contraction. Simultaneous $Ca^{2+}$ transients (CaT) were recorded using Fura-2 dual-wavelength ratiometric method[12], which is more precise than the Fluo-4 single-wavelength method.

The recording solution contained (in mM): 145 NaCl, 4 KCl, 1 $CaCl_2$, 0.33 $NaH_2PO_4$, 1 $MgCl_2$, 10 Glucose, 10 HEPES, with pH 7.4. In a separate set of experiments, $HCO_3^-$ was used as a buffer, and the recording solution contained (in mM): 120 NaCl, 4 KCl, 1 $CaCl_2$, 0.33 $NaH_2PO_4$, 1 $MgCl_2$, 10 Glucose, 24 $NaHCO_3$, gassed by 5% $CO_2$ and 95% $O_2$. To reduce the $pH_i$, but keep $pH_o$ constant, sodium acetate was applied to clamp the $pH_i$[13, 14]. Sodium acetate was used to replace an equal concentration of NaCl, and 5 μM 5-(N-Ethyl-N-isopropyl) amiloride (EIPA) was added to inhibit the $Na^+/H^+$ exchanger for acetate application.

### Intracellular pH ($pH_i$) measurement

The $pH_i$ of cardiomyocytes was measured using carboxy-SNARF-1 fluorescent pH indicator. Isolated cardiomyocytes were loaded with 10 μM SNARF-1 AM in Tyrode's solution. The measurement was performed using $Na^+$-free solutions, buffered by either HEPES or $HCO_3^-$. HEPES-buffered solution contained (in mM): 144 NMG-Cl, 4 KCl, 1 $MgCl_2$, 2 $CaCl_2$, 10 Glucose, 10 HEPES, and pH 7.4. $HCO_3^-$-buffered solution contained (in mM): 120 NMG-Cl, 4 KCl, 1 $MgCl_2$, 2 $CaCl_2$, 10 Glucose, 24 Choline-$HCO_3$, gassed by 5% $CO_2$ and 95% $O_2$. Sodium acetate was used to clamp $pH_i$, and 5 μM 5-(N-Ethyl-N-isopropyl) amiloride (EIPA) was added to inhibit the $Na^+/H^+$ exchanger for acetate application.

The SNARF emission ratio ($F_{580}/F_{640}$) was converted to $pH_i$ using standard calibration[15–17]. SNARF emission ratios were measured while cells were perfused by calibration solutions with five different pH values. The calibration solutions contained (in mM): 140 KCl, 1

$MgCl_2$, 20 HEPES (or MES at pH 5.5), with pH 5.5, 6.5, 7.0, 7.5, and 8.0. Negericin (10 μM, a $K^+/H^+$ antiporter ionophore) was added to the calibration solution before use.

### Molecular cloning from human cardiac tissues

De-identified human ventricular specimens were obtained from a commercial source (T Cubed), in accordance with the approved UC Davis Institutional Review Board (IRB) protocol. Total RNA and mRNA were extracted, and similar cloning strategy was used as previously described[7].

### Heterologous expression in Chinese hamster ovary (CHO) cells

Human cardiac SLC26A6 isoforms were expressed in CHO cells following the protocol we used previously[7].

### Statistical analyses

Data are presented as mean ± S.E.M. Statistical comparisons were analyzed by student's t-test. Statistical significance was considered to be achieved when $p<0.05$.

## Results

### Ablation of *Slc26a6*$^{-/-}$ results in cardiac AP shortening

To test the functional roles of Slc26a6, we took advantage of an *Slc26a6*$^{-/-}$ mouse model.[8] We first confirmed the lack of Slc26a6 expression in ventricular myocytes isolated from *Slc26a6*$^{-/-}$ mice (Fig. 1A), and the two bands in WT lane suggest different mouse cardiac slc26a6 isoforms we reported before[7]. To test the role of Slc26a6 in $Cl^-/HCO_3^-$ and $Cl^-$/oxalate exchange, we recorded outward currents using fast solution exchange and suspended whole-cell recording methods, as we have previously described.[7] Fig. 1B&C show the solution exchange configuration and corresponding currents, respectively, recorded from WT and *Slc26a6*$^{-/-}$ ventricular myocytes. The outward $Cl^-/HCO_3^-$ and $Cl^-$/oxalate exchange currents were completely abolished in *Slc26a6*$^{-/-}$ ventricular myocytes (Fig. 1C, right).

Since cardiac Slc26a6 is an electrogenic $Cl^-/HCO_3^-$ exchanger, we predict that activities of Slc26a6 will affect cardiac APDs. There were no significant differences in the resting membrane potentials (RMPs), however, APD at 90% repolarization ($APD_{90}$) was significantly shorter in *Slc26a6*$^{-/-}$ ventricular myocytes compared to WT (Fig. 1D, E and F). It has previously been reported that the stoichiometry of cardiac Slc26a6 for $HCO_3^-$:$Cl^-$ is 2 or greater, therefore, the estimated reversal potential of the exchange is ~+36 mV under physiological condition. Our findings are consistent with the prediction that Slc26a6 generates inward currents by electrogenic $Cl^-/HCO_3^-$ exchange through most of the AP, due to the positive reversal potential for $Cl^-/HCO_3^-$ exchange under physiological condition in cardiomyocytes.[7] Indeed, a prominent inward current can be generated in cardiomyocytes *via* $Cl^-/HCO_3^-$ exchange with 24 mM $HCO_3^-$ inside the cells (Fig. 1G).

The APD shortening may also be caused by the remodeling of other major ion channels such as $Ca^{2+}$ and $K^+$ channels due to the knockout of *Slc26a6*. We therefore recorded the $Ca^{2+}$

and total $K^+$ currents from WT and *Slc26a6*$^{-/-}$ ventricular myocytes. As shown in supplemental Figure 2, we did not find significant differences in the current density between WT and *Slc26a6*$^{-/-}$ myocytes.

### *Slc26a6*$^{-/-}$ cardiomyocytes show reduced sarcomere shortening, $Ca^{2+}$ transient, and SR $Ca^{2+}$ load

The shortening of cardiac APs in *Slc26a6*$^{-/-}$ is predicted to result in decreased $Ca^{2+}$ entry and possible impairment of cardiomyocyte contractility. We, therefore, tested the $Ca^{2+}$ transient (CaT), sarcomere shortening, and SR $Ca^{2+}$ load in WT and *Slc26a6*$^{-/-}$ ventricular myocytes using HEPES ($Cl^-/OH^-$ exchange, Fig 2A–D) or $HCO_3^-$ ($Cl^-/HCO_3^-$ exchange, Fig. 2E–H) buffered solutions. Compared to WT cardiomyocytes, *Slc26a6*$^{-/-}$ cardiomyocytes demonstrated significantly reduced fractional shortening and CaT amplitude (Fig. 2A&B). To test whether the decrease in CaT was due to reduced SR $Ca^{2+}$ content, we measured the SR $Ca^{2+}$ content in WT and *Slc26a6*$^{-/-}$ cardiomyocytes (Fig. 2C&D). Indeed, the SR $Ca^{2+}$ load was significantly reduced in *Slc26a6*$^{-/-}$ cardiomyocytes. Similar findings are shown for $HCO_3^-$ buffered solution (Fig. 2E–H).

### Roles of Slc26a6 in $pH_i$ regulation

To test whether the $Cl^-/HCO_3^-$ exchange, mediated by Slc26a6, contributes to $pH_i$ regulation in ventricular myocytes, we directly measured the $pH_i$ of cardiomyocytes by using SNARF-1 AM pH dye, as shown in Fig. 3A and *B*. The $pH_i$ in resting *Slc26a6*$^{-/-}$ cardiomyocytes was 7.42 ± 0.02, significantly higher than that of 7.16 ± 0.02 in WT cardiomyocytes (n=5, *$p$<0.05). To test the function of Slc26a6 in acid loading, we first induced intracellular acidification by wash in of 40 mM acetate followed by an immediate wash out, and monitored the $pH_i$ recovery from alkalization. The $pH_i$ in WT cardiomyocytes recovered to the baseline level over time (Fig. 3C), whereas there was a delay in the recovery of $pH_i$ in *Slc26a6*$^{-/-}$ cardiomyocytes, over the same period of time (Fig. 3D). The results suggested an impairment of the acidification process in *Slc26a6*$^{-/-}$ cardiomyocytes and participation of Slc26a6 in the acid loading in cardiomyocytes.

We reason, based on its exchange activities, that Slc26a6 contributes to acid loading in cardiomyocytes under normal physiological condition, and that ablation of Slc26a6 may delay the acid loading process and affect the sarcomere shortening and CaT. We perfused ventricular myocytes with a solution containing 40 mM sodium acetate to acidify the cytosol, and monitored the sarcomere shortening and CaT, as shown in Fig. 3E. Acid loading resulted in marked reduction of sarcomere shortening in both WT and *Slc26a6*$^{-/-}$. The CaT was initially enhanced slightly, and then inhibited by acetate-induced intracellular acidification. Moreover, after wash out of acetate, the recovery process of sarcomere shortening and CaT was much slower in *Slc26a6*$^{-/-}$ cardiomyocytes, consistent with Slc26a6 exchange activities (please note that different scales were used for upper and lower panels). The immediate alkalization during the wash out of acetate also inhibited contraction of the cardiomyocytes.

### A decrease in fractional shortening in *Slc26a6*$^{-/-}$ mice

The above cellular data strongly support the contributions of Slc26a6 to cardiac $pH_i$, APD, and contractility. To test the effects of reduced CaT and sarcomere shortening in *Slc26a6*$^{-/-}$ on *in vivo* cardiac function, we performed echocardiography in conscious mice. There was no evidence of cardiac hypertrophy or dilation, with no significant differences in heart/body weight ratios between WT and *Slc26a6*$^{-/-}$ mice (Fig. 4A&B). However, *Slc26a6*$^{-/-}$ mice showed evidence of sinus bradycardia (Fig. 4C). Histological analyses, using wheat germ agglutinin and Picrosirius Red stain, of cardiac sections demonstrated no evidence of cardiac fibrosis, hypertrophy, or dilation in *Slc26a6*$^{-/-}$ mice (Fig. 4D). However, there was a significant reduction in the fractional shortening in *Slc26a6*$^{-/-}$ mice compared to WT controls (Fig. 4E).

Indeed, hemodynamic monitoring demonstrated a significant decrease in cardiac contractility in *Slc26a6*$^{-/-}$ mice compared to WT controls. Shown in Fig. 5A are representative recordings of left ventricular pressure, volume, and developed pressure (dP/dt) in WT and *Slc26a6*$^{-/-}$ mice. There was a significant right and downward shift of the pressure-volume (P-V) loops in *Slc26a6*$^{-/-}$ mice, indicating reduced end systolic pressure and relatively larger end systolic and diastolic volumes, with reduced stroke volume (Fig. 5B). To determine the end systolic P-V relationship, we obtained a series of P-V loops by altering the preload and derived the slope of the end systolic P-V relationship (Ees), a load independent measure of cardiac contractility (Fig. 5C&D for WT and *Slc26a6*$^{-/-}$, respectively). Consistent with the cellular data and echocardiography data, the end systolic pressure (Fig. 5E), maximum dP/dt (Fig. 5F), and Ees (Fig. 5G) in *Slc26a6*$^{-/-}$ mice were significantly reduced compared to those of WT mice, supporting a decrease in cardiac contractility in *Slc26a6*$^{-/-}$ mice.

### Fragmented QRS complex in *Slc26a6*$^{-/-}$ mice

Cellular electrophysiology and $pH_i$ measurement of *Slc26a6*$^{-/-}$ cardiomyocytes demonstrated the shortening of $APD_{90}$ and an elevated $pH_i$ (Fig. 1 & 3). We, therefore, compared the ECG between WT and *Slc26a6*$^{-/-}$ mice (Fig. 6A&B). *Slc26a6*$^{-/-}$ mice showed evidence of fragmented QRS complex with prolonged PR interval. The QRS complex duration of *Slc26a6*$^{-/-}$ mice was significantly prolonged compared to that of WT mice (22.8 ± 0.8 ms *vs* 20.3 ± 0.5 ms; n=8, $p< 0.05$). Mice were challenged with subcutaneous isoproterenol (ISO, 25 mg/kg, Fig. 6C&D). ISO injection increased heart rates, but fragmented QRS complexes remained in *Slc26a6*$^{-/-}$ mice. Summary data are shown in Fig. 6E&F. Of note, even though the heart rate measured by echocardiography was significantly reduced in unanesthesized *Slc26a6*$^{-/-}$ compared to WT mice (Fig. 4C), only the PR intervals were significantly prolonged in the anesthetized *Slc26a6*$^{-/-}$ mice during ECG recordings (Fig. 6E). These *in vivo* findings suggest critical roles of Slc26a6 in cardiac conduction systems that warrant additional future investigations.

### Molecular identification of human cardiac SLC26A6 isoforms

Previous studies suggest that $Cl^-$/oxalate exchange of mouse Slc26a6 is electrogenic, while the human SLC26A6 mediates electroneutral $Cl^-$/oxalate exchange.[18, 19] To directly test

whether there are indeed species differences, we performed RT-PCR to clone full-length SLC26A6 from human heart (Fig. 7).

Six different transcript variants of human SLC26A6 have previously been described. During the cloning of human cardiac SLC26A6, two major transcript variants were repetitively obtained, suggesting the presence of alternatively spliced variants of SLC26A6 in human heart. We used a For-long and Rev primer set, as well as a For-short and Rev primer set (Fig. 7A); the PCR products were shown in Fig. 7B. 12 clones were randomly selected for each primer set, compared by restriction enzyme digestion, and full-length sequence confirmed by sequencing. Sequence analysis revealed that the two identified isoforms correspond to previously described transcript variant 2 (NM_134263.2) and transcript variant 4 (NM_001040454.1) for primer set 1 and 2, respectively. Variant 4 is 21 amino acids shorter in the N-terminus compared to transcript variant 2 (see protein sequence alignment in Supplementary Figure 3).

### Electrogenic $Cl^-$/oxalate and $Cl^-/HCO_3^-$ exchange activities mediated by human cardiac SLC26A6 isoforms

To test the function of the human cardiac SLC26A6, we expressed the human cardiac SLC26A6 isoforms in CHO cells and recorded the current generated by the anion exchanger, using patch-clamp coupled with a fast solution exchange technique, as described in Fig. 1B &G. Membrane potential was held at 0 mV. Fig. 7C shows the outward currents generated by electrogenic $Cl^-$/oxalate and $Cl^-/HCO_3^-$ exchanges, and the inward currents generated by $Cl^-/HCO_3^-$ exchanges. Both variants identified in human hearts are functional electrogenic $Cl^-$/oxalate and $Cl^-/HCO_3^-$ exchangers.

## Discussion

Slc26a6 has been proposed to be the predominant $Cl^-/HCO_3^-$ exchanger and a specific $Cl^-/OH^-$ exchanger in the mouse heart, based on transcript levels.[6] Our group has since identified four cardiac Slc26a6 isoforms in the mouse heart, and importantly, we demonstrated that mouse cardiac Slc26a6 mediates eletrogenic $Cl^-/HCO_3^-$ exchange activities in cardiac myocytes.[7] We predict, based on its electrogenic activities, that Slc26a6 may participate not only in the regulation of $pH_i$, but also in cardiac excitability. To directly test this hypothesis, we took advantage of *Slc26a6*$^{-/-}$ mice. Consistent with our prediction, ablation of *Slc26a6* significantly shortens APD, resulting in reduced sarcomere shortening, CaT, and SR $Ca^{2+}$ load, in addition to an elevated $pH_i$. Moreover, our *in vivo* studies demonstrate decreased fractional shortening and cardiac contractility, as well as sinus bradycardia in the knockout mice. For the first time, our results uncover new insights into the critical roles of cardiac electrogenic anion transporter—linking the regulation of not only $pH_i$, but also cardiac excitability and contractility.

### Roles of bicarbonate in cardiac pH regulation

$HCO_3^-/CO_2$ buffer is the major component of the cellular pH buffering system. Bicarbonate is the byproduct of mitochondrial respiration; therefore, its concentration is highly affected by physiological and pathological conditions. $HCO_3^-$ is critical for pH regulation, acid/base

secretion, and body fluid secretion.[20, 21] Although $CO_2$ can diffuse across the plasma membrane, $HCO_3^-$ transport across the plasma membrane requires facilitation by $HCO_3^-$ transporters and anion channels. $HCO_3^-$ transporters are encoded by 14 genes belonging to *SLC4A* and *SLC26A* gene families.[20]

The heart is an organ with a high metabolic rate, due to its continuous mechanical activities. Therefore, $HCO_3^-$ is a critical anion in the regulation of cardiac function[1, 2]. Unlike $Na^+$, $K^+$ and $Ca^{2+}$ ions, which directly affect the excitability and contractility of the heart, $HCO_3^-$ participates in the regulation of cardiac function through its coupled transport with other cations and anions, as well as its direct control of cardiac pH. Therefore, it is a unique anion in the heart with dynamic regulation and a wide range of function. $HCO_3^-$ participates in acid extruding and acid loading processes in cardiomyocytes, which are coupled with $Na^+$ and $Cl^-$ transport, respectively.[1] Our studies provided strong evidence to support the role of Slc26a6 as an acid loader contributing to the acid loading process in cardiomyocytes. Since cardiac Slc26a6 mediates $Cl^-/HCO_3^-$ and $Cl^-/OH^-$ exchange, our study also demonstrated the critical roles of $Cl^-$ in regulation of cardiac function through Slc26a6.

## Electrogenic properties of human SLC26A6

In contrast to our current findings, previous studies suggest that human SLC26A6 may not be electrogenic.[18, 19] These studies, however, used an oocyte expression system and indirect measurement of changes in reversal potentials, wherein intracellular ion concentrations were unknown and could not be precisely controlled during the recordings. In contrast, we used patch-clamp recordings with fast solution exchange to precisely set the ion gradient across the plasma membrane and monitor the dynamic changes of the currents. We observed electrogenic $Cl^-/HCO_3^-$ and $Cl^-$/oxalate exchange activities of both mouse and human cardiac SLC26A6 (Fig. 7).

## Critical roles of electrogenic transporters in cardiac excitability

Electrogenic transporters contribute significantly to cardiac excitability. The well described $Na^+/K^+$ pump contributes to the generation of resting membrane potentials and repolarization of cardiac action potentials.[22] Another electrogenic transporter, $Na^+/Ca^{2+}$ exchanger (NCX), is not only important in intracellular $Ca^{2+}$ homeostasis and cardiac contractility, but also in the regulation of cardiac excitability and arrhythmogenesis. Similar to *Slc26a6*$^{-/-}$, cardiac-specific NCX knockout mice show an abbreviated APD in cardiomyocytes.[23–25] Additionally, the electrogenic $Na^+/HCO_3^-$ cotransporter was reported to modulate resting membrane potentials and cardiac APs.[26]

Slc26a6 mediates eletrogenic $Cl^-/HCO_3^-$ exchange in the heart, thus regulating cardiac APD, as we demonstrate for the first time in this study. Based on the predicted stoichiometry of Slc26a6, at least two $HCO_3^-$ are exchanged for one $Cl^-$ ion, with estimated reversal potential of the exchange of ~+36 mV. Under physiological condition, the activation of Slc26a6 generates inward currents, which depolarize the membrane potential.[7] Consistently, *Slc26a6*$^{-/-}$ cardiomyocytes show shortened cardiac APs.

### Functional roles of Slc26a6 in acid loading process in cardiomyocytes

The elevated $pH_i$ in *Slc26a6*$^{-/-}$ cardiomyocytes supports the essential role of Slc26a6 in the acid loading process.[1, 2, 6, 7] Under physiological conditions, Slc26a6 mediates $Cl^-/HCO_3^-$ or $Cl^-/OH^-$ exchange, maintaining a relatively lower $pH_i$ and higher intracellular $Cl^-$ concentration in cardiomyocytes. Here, we directly monitored the acidification process during the application and wash out of acetate. *Slc26a6*$^{-/-}$ cardiomyocytes show delayed acidification, supporting the role of Slc26a6 in cellular acid loading (Fig. 3).

In addition to Slc26a6, it has been reported that Slc4a families are expressed in cardiomyocytes, including AE1 (Slc4a1), AE2 (Slc4a2), and AE3 (Slc4a3), which are acid loaders. Other Slc4a members are mostly $Na^+/HCO_3^-$ cotransporters, mediating acid extrusion. However, the expression levels of AE1, AE2, AE3, as well as Slc26a3 are relatively low compared to Slc26a6.[6] Nonetheless, it is possible that there is compensation from AE and other Slc26a families during the $pH_i$ recovery process. The dominant molecule for acid loading is Slc26a6 because its expression level is nearly one hundred fold higher than that of AEs and Slc26a3.

### Decreased cardiac contractility in *Slc26a6*$^{-/-}$ mice

The shortened cardiac APs are predicted to decrease $Ca^{2+}$ influx through L-type $Ca^{2+}$ channels, leading to reduced CaT and sarcomere fractional shortening in *Slc26a6*$^{-/-}$ cardiomyocytes. Additionally, the elevated $pH_i$ may contribute to changes in CaT and contractility. Indeed, $pH_i$ is a critical regulator of cardiac ion channels and transporters, as well as other membrane and contractile proteins, and, therefore, exerts significant influences on cardiac $Ca^{2+}$ signaling, contractility, and excitability.[1, 2] Effects of acidosis on cardiac function have been extensively investigated due to its pathological significance during ischemia-reperfusion.[27–34] Cellular acidification reduces CaT and contraction in cardiomyocytes.[1, 27, 29, 31, 35] Our results showed that CaT was initially enhanced and later inhibited by cellular acidification, induced by wash in of acetate (Fig. 3E) when $Na^+/H^+$ exchanger was inhibited, similar to that observed by Vaughan-Jones et al.[1] The reduced sarcomere shortening observed in our study from acidification (Fig. 3E), agrees with previously reported findings.

On the other hand, effects of intracellular alkalization on cardiac contractility and CaT are less understood. Our findings in Fig. 3E demonstrate that acid loading had a relatively small influence on CaT compared to cell shortening in both WT and *Slc26a6*$^{-/-}$ myocytes, however, alkalization during wash out dramatically decreased CaT and cell shortening. The findings suggest that lower $pH_i$ had a minor effect on CaT, but may affect the $Ca^{2+}$ affinity of troponin C.[1] Taken together, the impairment of cardiac contractility in *Slc26a6*$^{-/-}$ mice is likely due to multiple mechanisms, including alterations in $pH_i$, in addition to reduced APDs, CaT, and SR $Ca^{2+}$ load.

### Future studies

One previous study using a different strain of *Slc26a6*$^{-/-}$ mice reported normal body weight, heart rate, and blood pressure in *Slc26a6*$^{-/-}$ mice.[36] Our studies demonstrate comparable heart/body weight ratio between WT and *Slc26a6*$^{-/-}$ mice, however, there is evidence of

sinus bradycardia and fragmented QRS complex in *Slc26a6*$^{-/-}$ mice with prolonged PR interval. Fragmented QRS complexes have been shown to be common in patients post myocardial infarction; they may represent a marker for cardiovascular diseases[37–39], and predict arrhythmic events and mortality in patients with cardiomyopathy.[40, 41] Fragmented QRS was also reported to be associated with prognosis in patients with Brugada syndrome, supporting the association of fragmented QRS and arrhythmia substrate.[42] *Slc26a6*$^{-/-}$ mice showed sinus bradycardia and fragmented QRS, however, there is no significant cardiac fibrosis in *Slc26a6*$^{-/-}$ mice. Our findings of fragmented QRS complexes and prolonged PR interval in *Slc26a6*$^{-/-}$ mice support the critical role of Slc26a6 not only in ventricular myocytes, but also in the cardiac conduction system. Sinus bradycardia in *Slc26a6*$^{-/-}$ mice further suggests functional roles of Slc26a6 in pacemaking cells.

In addition, the elevated $pH_i$ may result in changes in gene expression profiles, as well as the function of other membrane and cytosolic proteins. For example, $pH_i$ may affect APDs of rabbit and guinea pig ventricular myocytes by $H^+$-induced changes in late $Ca^{2+}$ entry through the L-type $Ca^{2+}$ channel.[43] Therefore, we expect a spectrum of cellular proteins which need to be further evaluated. However, these extensive investigations will be performed in our future experiments.

The global knockout of *Slc26a6* was reported to affect the kidney and duodenum epithelial transport[36] and induce $Ca^{2+}$ oxalate urolithiasis.[8] The alteration in metabolic profiles in *Slc26a6*$^{-/-}$ may affect the observed *in vivo* cardiac function. Therefore, we took advantage of not only *in vivo* physiological measurement, but also *in vitro* analyses in our studies to circumvent these possible confounding factors. Indeed, our *in vivo* findings are consistent with *in vitro* analyses.

In conclusion, the *in vivo* and *in vitro* studies unravel novel mechanistic insights into the newly described and unique cardiac electrogenic $Cl^-/HCO_3^-$ transporter in ventricular myocytes. Activities of Slc26a6 contribute not only to the regulation of $pH_i$, but also cardiac AP and contractility. Ablation of *Slc26a6* shortens the APDs, impairs cardiac function, and results in fragmented QRS complexes and elevated $pH_i$. Additional studies are required to further understand the functional roles of Slc26a6 not only in ventricular myocytes, but also in pacemaking cells and the cardiac conduction system.

## Supplementary Material

Refer to Web version on PubMed Central for supplementary material.

## Acknowledgments

We thank Dr. Peter S. Aronson (Yale University) for his kind gift of *Slc26a6* knockout mice and reading of our manuscript.

**Sources of Funding:** This study was supported, in part, by American Heart Association Beginning Grant-in-Aid 14BGIA18870087 (Dr Zhang), National Institutes of Health (NIH) R01 DC015135, NIH R01 DC015252, NIH R01 DC016099, and NIH P01 AG051443 (Dr Yamoah), NIH R01 HL123526 (Dr Chen-Izu), NIH R01 HL085727, NIH R01 HL085844, NIH R01 HL137228, and S10 RR033106 (Dr Chiamvimonvat), VA Merit Review Grant I01 BX000576 and I01 CX001490 (Dr Chiamvimonvat), and American Heart Association Postdoctoral Fellowship Award (Dr Sirish). Dr Sirish received Postdoctoral Fellowship from California Institute for Regenerative Medicine Training Grant to UC Davis and NIH/National Heart, Lung and Blood Institute (NHLBI) Institutional Training

Grant in Basic and Translational Cardiovascular Science (T32 NIH HL086350). H.A. Ledford and R. Shimkunas received Predoctoral Fellowship from NIH/NHLBI Institutional Training Grant in Basic and Translational Cardiovascular Science (T32 NIH HL086350) and NIH F31 Predoctoral Awards. M. Moshref received Predoctoral Fellowship from the Training Core of the NIH/National Institute of Environmental Health Sciences (NIEHS) UC Davis Superfund Program (P42 NIH ES004699). Dr Chiamvimonvat is the holder of the Roger Tatarian Endowed Professorship in Cardiovascular Medicine, University of California, Davis and a Staff Cardiologist, VA Medical Center, Mather, CA.

## References

1. Vaughan-Jones RD, Spitzer KW, Swietach P. Intracellular pH regulation in heart. J Mol Cell Cardiol. 2009; 46:318–331. [PubMed: 19041875]
2. Wang HS, Chen Y, Vairamani K, Shull GE. Critical role of bicarbonate and bicarbonate transporters in cardiac function. World journal of biological chemistry. 2014; 5:334–345. [PubMed: 25225601]
3. Mount DB, Romero MF. The slc26 gene family of multifunctional anion exchangers. Pflugers Arch. 2004; 447:710–721. [PubMed: 12759755]
4. Dorwart MR, Shcheynikov N, Yang D, Muallem S. The solute carrier 26 family of proteins in epithelial ion transport. Physiology (Bethesda). 2008; 23:104–114. [PubMed: 18400693]
5. Alper SL, Sharma AK. The slc26 gene family of anion transporters and channels. Molecular aspects of medicine. 2013; 34:494–515. [PubMed: 23506885]
6. Alvarez BV, Kieller DM, Quon AL, Markovich D, Casey JR. Slc26a6: A cardiac chloride-hydroxyl exchanger and predominant chloride-bicarbonate exchanger of the mouse heart. J Physiol. 2004; 561:721–734. [PubMed: 15498800]
7. Kim HJ, Myers R, Sihn CR, Rafizadeh S, Zhang XD. Slc26a6 functions as an electrogenic $Cl^-$/$HCO_3^-$ exchanger in cardiac myocytes. Cardiovascular Research. 2013; 100:383–391. [PubMed: 23933580]
8. Jiang Z, Asplin JR, Evan AP, Rajendran VM, Velazquez H, Nottoli TP, Binder HJ, Aronson PS. Calcium oxalate urolithiasis in mice lacking anion transporter slc26a6. Nat Genet. 2006; 38:474–478. [PubMed: 16532010]
9. Sirish P, Li N, Timofeyev V, Zhang XD, Wang L, Yang J, Lee KS, Bettaieb A, Ma SM, Lee JH, Su D, Lau VC, Myers RE, Lieu DK, Lopez JE, Young JN, Yamoah EN, Haj F, Ripplinger CM, Hammock BD, Chiamvimonvat N. Molecular mechanisms and new treatment paradigm for atrial fibrillation. Circ Arrhythm Electrophysiol. 2016:9.
10. Zhang XD, Timofeyev V, Li N, Myers RE, Zhang DM, Singapuri A, Lau VC, Bond CT, Adelman J, Lieu DK, Chiamvimonvat N. Critical roles of a small conductance $Ca^{2+}$-activated $K^+$ channel (SK3) in the repolarization process of atrial myocytes. Cardiovascular Research. 2014; 101:317–325. [PubMed: 24282291]
11. Mitchell GF, Jeron A, Koren G. Measurement of heart rate and Q-T interval in the conscious mouse. Am J Physiol. 1998; 274:H747–751. [PubMed: 9530184]
12. Jian Z, Han H, Zhang T, Puglisi J, Izu LT, Shaw JA, Onofiok E, Erickson JR, Chen YJ, Horvath B, Shimkunas R, Xiao W, Li Y, Pan T, Chan J, Banyasz T, Tardiff JC, Chiamvimonvat N, Bers DM, Lam KS, Chen-Izu Y. Mechanochemotransduction during cardiomyocyte contraction is mediated by localized nitric oxide signaling. Science signaling. 2014; 7:ra27. [PubMed: 24643800]
13. Thomas RC. Experimental displacement of intracellular pH and the mechanism of its subsequent recovery. J Physiol. 1984; 354:3P–22P.
14. Roos A, Boron WF. Intracellular pH. Physiol Rev. 1981; 61:296–434. [PubMed: 7012859]
15. Buckler KJ, Vaughan-Jones RD. Application of a new pH-sensitive fluoroprobe (carboxy-snarf-1) for intracellular pH measurement in small, isolated cells. Pflugers Arch. 1990; 417:234–239. [PubMed: 2084617]
16. Blank PS, Silverman HS, Chung OY, Hogue BA, Stern MD, Hansford RG, Lakatta EG, Capogrossi MC. Cytosolic pH measurements in single cardiac myocytes using carboxy-seminaphthorhodafluor-1. Am J Physiol. 1992; 263:H276–284. [PubMed: 1636765]
17. Niederer SA, Swietach P, Wilson DA, Smith NP, Vaughan-Jones RD. Measuring and modeling chloride-hydroxyl exchange in the guinea-pig ventricular myocyte. Biophys J. 2008; 94:2385–2403. [PubMed: 18055536]

18. Chernova MN, Jiang L, Friedman DJ, Darman RB, Lohi H, Kere J, Vandorpe DH, Alper SL. Functional comparison of mouse slc26a6 anion exchanger with human SLC26A6 polypeptide variants: Differences in anion selectivity, regulation, and electrogenicity. J Biol Chem. 2005; 280:8564–8580. [PubMed: 15548529]
19. Clark JS, Vandorpe DH, Chernova MN, Heneghan JF, Stewart AK, Alper SL. Species differences in $Cl^-$ affinity and in electrogenicity of slc26a6-mediated oxalate/$Cl^-$ exchange correlate with the distinct human and mouse susceptibilities to nephrolithiasis. J Physiol. 2008; 586:1291–1306. [PubMed: 18174209]
20. Cordat E, Casey JR. Bicarbonate transport in cell physiology and disease. Biochem J. 2009; 417:423–439. [PubMed: 19099540]
21. Casey JR, Grinstein S, Orlowski J. Sensors and regulators of intracellular pH. Nat Rev Mol Cell Biol. 2010; 11:50–61. [PubMed: 19997129]
22. Bueno-Orovio A, Sanchez C, Pueyo E, Rodriguez B. $Na^+/K^+$ pump regulation of cardiac repolarization: Insights from a systems biology approach. Pflugers Arch. 2014; 466:183–193. [PubMed: 23674099]
23. Pott C, Henderson SA, Goldhaber JI, Philipson KD. $Na^+/Ca^{2+}$ exchanger knockout mice: Plasticity of cardiac excitation-contraction coupling. Ann N Y Acad Sci. 2007; 1099:270–275. [PubMed: 17446467]
24. Pott C, Ren X, Tran DX, Yang MJ, Henderson S, Jordan MC, Roos KP, Garfinkel A, Philipson KD, Goldhaber JI. Mechanism of shortened action potential duration in $Na^+$-$Ca^{2+}$ exchanger knockout mice. Am J Physiol Cell Physiol. 2007; 292:C968–973. [PubMed: 16943244]
25. Pott C, Philipson KD, Goldhaber JI. Excitation-contraction coupling in $Na^+$-$Ca^{2+}$ exchanger knockout mice: Reduced transsarcolemmal $Ca^{2+}$ flux. Circ Res. 2005; 97:1288–1295. [PubMed: 16293789]
26. Villa-Abrille MC, Petroff MG, Aiello EA. The electrogenic $Na^+/HCO_3^-$ cotransport modulates resting membrane potential and action potential duration in cat ventricular myocytes. J Physiol. 2007; 578:819–829. [PubMed: 17138608]
27. Bountra C, Vaughan-Jones RD. Effect of intracellular and extracellular pH on contraction in isolated, mammalian cardiac muscle. J Physiol. 1989; 418:163–187. [PubMed: 2621616]
28. Vaughan-Jones RD, Wu ML, Bountra C. Sodium-hydrogen exchange and its role in controlling contractility during acidosis in cardiac muscle. Mol Cell Biochem. 1989; 89:157–162. [PubMed: 2554122]
29. Orchard CH, Kentish JC. Effects of changes of pH on the contractile function of cardiac muscle. Am J Physiol. 1990; 258:C967–981. [PubMed: 2193525]
30. Harrison SM, Frampton JE, McCall E, Boyett MR, Orchard CH. Contraction and intracellular $Ca^{2+}$, $Na^+$, and $H^+$ during acidosis in rat ventricular myocytes. Am J Physiol. 1992; 262:C348–357. [PubMed: 1539627]
31. Fabiato A, Fabiato F. Effects of pH on the myofilaments and the sarcoplasmic reticulum of skinned cells from cardiace and skeletal muscles. J Physiol. 1978; 276:233–255. [PubMed: 25957]
32. Steenbergen C, Deleeuw G, Rich T, Williamson JR. Effects of acidosis and ischemia on contractility and intracellular pH of rat heart. Circ Res. 1977; 41:849–858. [PubMed: 21759]
33. Garlick PB, Radda GK, Seeley PJ. Studies of acidosis in the ischaemic heart by phosphorus nuclear magnetic resonance. Biochem J. 1979; 184:547–554. [PubMed: 44193]
34. Yan GX, Kleber AG. Changes in extracellular and intracellular pH in ischemic rabbit papillary muscle. Circ Res. 1992; 71:460–470. [PubMed: 1628400]
35. Choi HS, Trafford AW, Orchard CH, Eisner DA. The effect of acidosis on systolic $Ca^{2+}$ and sarcoplasmic reticulum calcium content in isolated rat ventricular myocytes. J Physiol. 2000; 529(Pt 3):661–668. [PubMed: 11118496]
36. Wang Z, Wang T, Petrovic S, Tuo B, Riederer B, Barone S, Lorenz JN, Seidler U, Aronson PS, Soleimani M. Renal and intestinal transport defects in slc26a6-null mice. Am J Physiol Cell Physiol. 2005; 288:C957–965. [PubMed: 15574486]
37. Flowers NC, Horan LG, Thomas JR, Tolleson WJ. The anatomic basis for high-frequency components in the electrocardiogram. Circulation. 1969; 39:531–539. [PubMed: 5778254]

38. Chatterjee S, Changawala N. Fragmented QRS complex: A novel marker of cardiovascular disease. Clinical cardiology. 2010; 33:68–71. [PubMed: 20186984]

39. Pietrasik G, Zareba W. QRS fragmentation: Diagnostic and prognostic significance. Cardiology journal. 2012; 19:114–121. [PubMed: 22461043]

40. Das MK, Maskoun W, Shen C, Michael MA, Suradi H, Desai M, Subbarao R, Bhakta D. Fragmented QRS on twelve-lead electrocardiogram predicts arrhythmic events in patients with ischemic and nonischemic cardiomyopathy. Heart Rhythm. 2010; 7:74–80. [PubMed: 20129288]

41. Das MK, Saha C, El Masry H, Peng J, Dandamudi G, Mahenthiran J, McHenry P, Zipes DP. Fragmented QRS on a 12-lead ECG: A predictor of mortality and cardiac events in patients with coronary artery disease. Heart Rhythm. 2007; 4:1385–1392. [PubMed: 17954396]

42. Morita H, Watanabe A, Morimoto Y, Kawada S, Tachibana M, Nakagawa K, Nishii N, Ito H. Distribution and prognostic significance of fragmented QRS in patients with brugada syndrome. Circ Arrhythm Electrophysiol. 2017:10.

43. Saegusa N, Moorhouse E, Vaughan-Jones RD, Spitzer KW. Influence of pH on $Ca^{2+}$ current and its control of electrical and $Ca^{2+}$ signaling in ventricular myocytes. J Gen Physiol. 2011; 138:537–559. [PubMed: 22042988]

**WHAT IS KNOWN?**

- Intracellular pH ($pH_i$) is critical to cardiac excitation and contraction. Uncompensated changes in $pH_i$ impair cardiac function and trigger arrhythmias, however, cardiac $pH_i$ regulation mechanisms are not completely understood.
- Our previous studies identified several isoforms of a solute carrier, Slc26a6, to be highly expressed in mouse cardiomyocytes. We demonstrated that Slc26a6 mediates electrogenic $Cl^-/HCO_3^-$ exchange activities in cardiomyocytes supporting the role of Slc26a6 in the regulation of $pH_i$ and cardiac function.

**WHAT THE STUDY ADDS?**

- Ablation of *Slc26a6* resulted in action potential (AP) shortening, reduced $Ca^{2+}$ transient and sarcoplasmic reticulum $Ca^{2+}$ load, decreased sarcomere shortening, and elevated $pH_i$ in mouse cardiomyocytes.
- At *in vivo* level, *Slc26a6* knockout mice showed reduced fractional shortening and cardiac contractility, as well as fragmented QRS complexes, supporting the critical roles of Slc26a6 in the regulation of cardiac excitability and contractility.
- For the first time, we identified human cardiac SLC26A6 isoforms and demonstrated their electrogenic $Cl^-/HCO_3^-$ exchange activities.

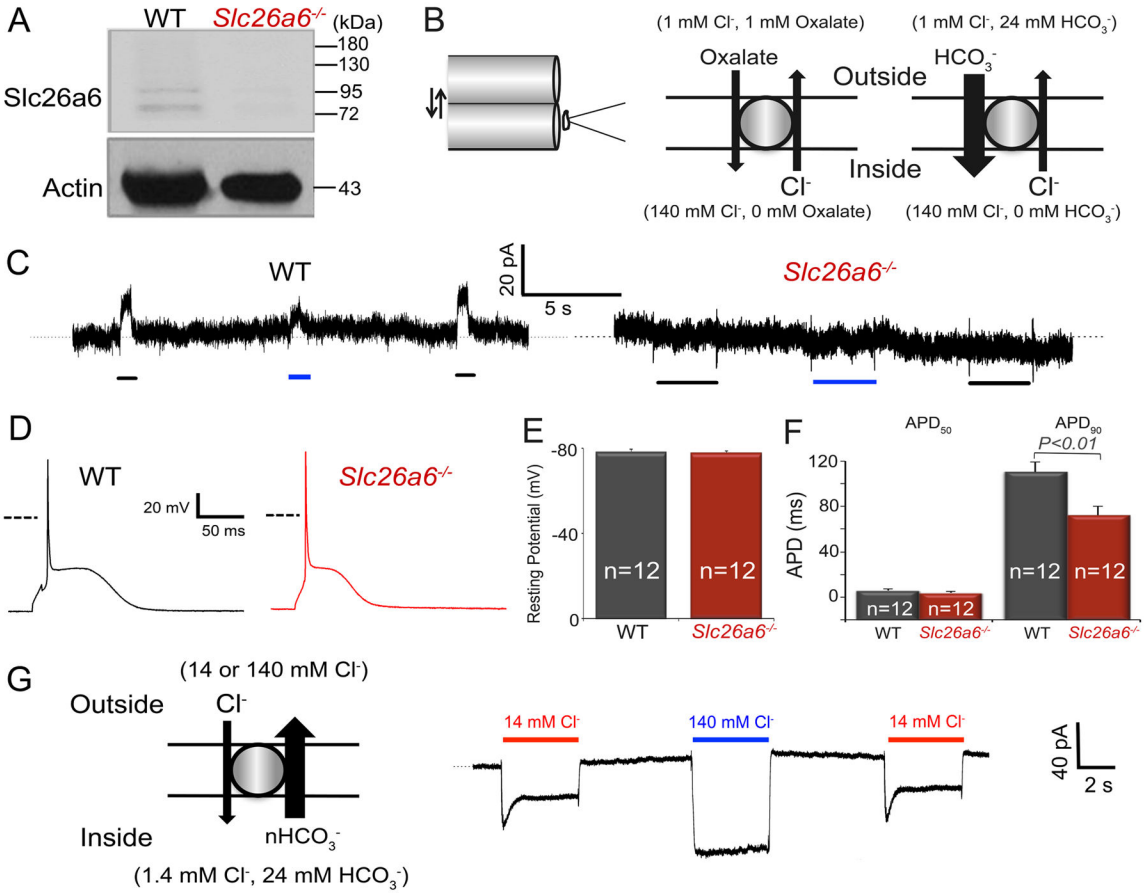


**Figure 1. Ablation of *Slc26a6*$^{-/-}$ results in cardiac AP shortening**

**A**. Western blot analysis confirms the absence of Slc26a6 expression in *Slc26a6*$^{-/-}$ mouse hearts. **B.** Schematic diagram of the fast solution exchange of the suspended whole-cell recording (left), and the ionic configuration to activate outward exchange current through Slc26a6. For recordings of the outward Slc26a6 currents, cardiomyocytes were first clamped at 0 mV, suspended, and moved to the outlet of the solution exchange capillary tube dispensing the bath control solution. Then the myocyte was switched to the capillary tube dispensing bath test solution, containing oxalate or $HCO_3^-$, for the activation of outward currents. The fast solution switch was performed by SF-77 solution exchanger controlled by pClamp10 software. The compositions of the bath control and test solutions have been described in Methods. **C**. Representative recording traces of outward currents recorded from WT ventricular myocytes (left) and *Slc26a6*$^{-/-}$ ventricular myocytes (right). The black and blue bars under the current traces represent the solution exchange to bath test solutions to activate $Cl^-$/Oxalate and $Cl^-/HCO_3^-$ exchange currents, respectively. **D**. Representative traces of action potentials (APs) from WT and *Slc26a6*$^{-/-}$ ventricular myocytes. Dashed lines represent 0 mV. **E**. Comparisons of resting membrane potentials (RMPs). **F**. Summary data of the action potential durations at 50% ($APD_{50}$) and 90% repolarization ($APD_{90}$). The AP and RMP were recorded in $HCO_3^-$ buffered bath solution. **G.** Inward $Cl^-/HCO_3^-$ exchange current elicited from WT ventricular myocytes using fast solution exchange, as indicated in the diagram on the left. The red and blue bars above the current traces represent

the solution exchange to bath test solutions containing 14 or 140 mM $Cl^-$ to activate $Cl^-/HCO_3^-$ exchange currents, respectively.

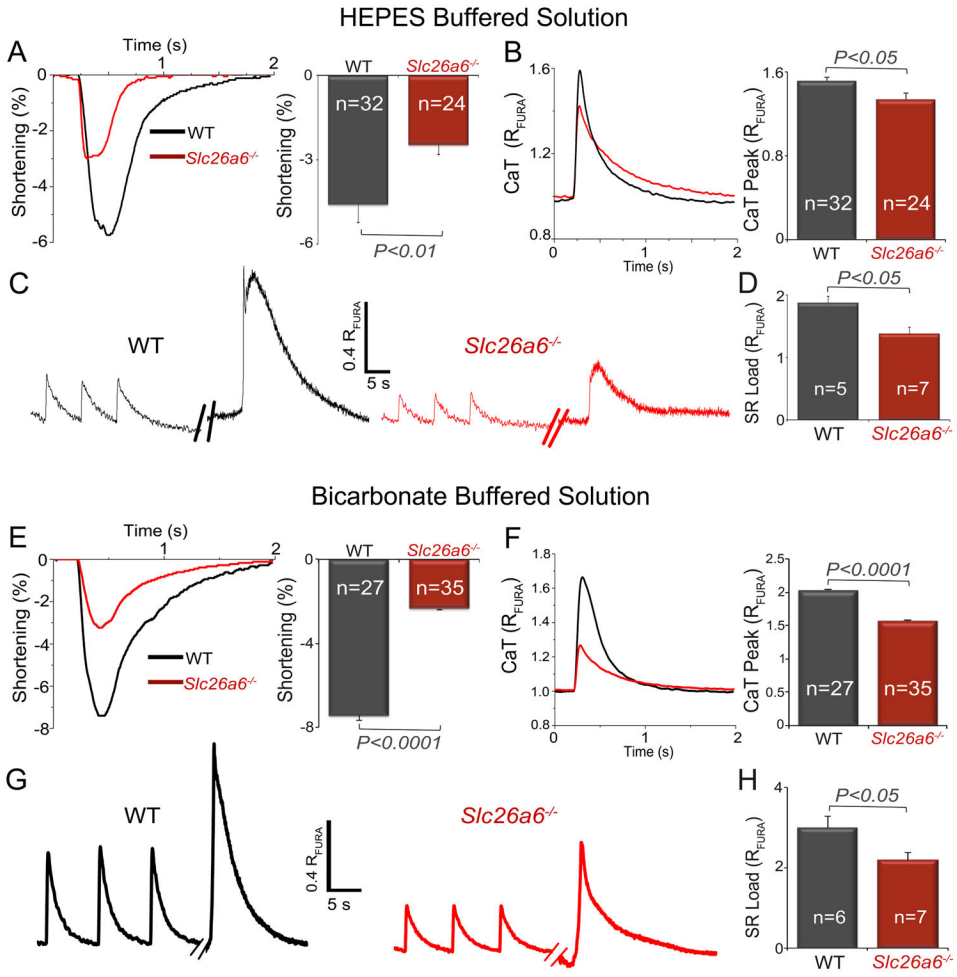


**Figure 2. *Slc26a6*$^{-/-}$ cardiomyocytes show reduced sarcomere shortening, $Ca^{2+}$ transient, and SR $Ca^{2+}$ load**

Experiments were performed using HEPES (panels **A–D**) or $HCO_3^-$ (panels **E–H**) as buffers. **A, E**. Representative traces and summary data for percentages of sarcomere shortening, and **B, F**. $Ca^{2+}$ transient (CaT) measured using Fura-2 ratio ($R_{FURA}$) from WT and *Slc26a6*$^{-/-}$ cardiomyocytes. **C, G**. Representative traces of sarcoplasmic reticulum (SR) $Ca^{2+}$ load measurement of WT and *Slc26a6*$^{-/-}$ ventricular myocytes. The myocytes were first paced to steady state, and then pacing was stopped for 15 s followed by a rapid application of 20 mM caffeine to induce SR $Ca^{2+}$ release. **D, H**. Summary data for SR $Ca^{2+}$ load from WT and *Slc26a6*$^{-/-}$ ventricular myocytes. Numbers within the bar graphs represent the sample sizes.

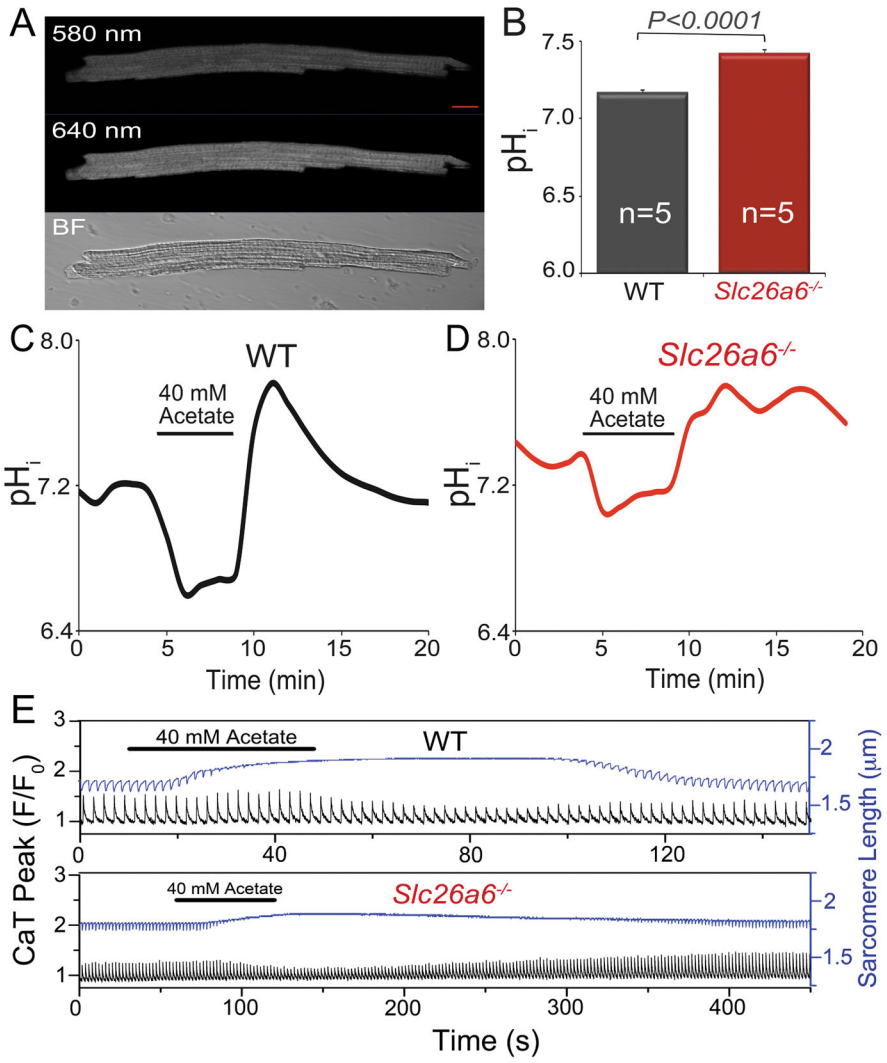


**Figure 3. *Slc26a6*$^{-/-}$ cardiomyocytes show higher intracellular pH ($pH_i$)**

**A**. Measurement of $pH_i$ in ventricular myocytes by SNARF-1 AM using confocal microscopy (scale bar: 10 μm). Loaded cells were excited by 488 nm laser and images were acquired by using two band-pass filters with center wavelengths of 580 nm and 640 nm, respectively. The ratio of the emission signals at 580 nm and 640 nm was calculated and converted to pH value following the standard methods described before[15–17]. A bright field (BF) image of the cardiomyocyte was also shown at the lower panel. **B**. Comparisons of $pH_i$ between WT and *Slc26a6*$^{-/-}$ cardiomyocytes. Alternations and recoveries of $pH_i$ when 40 mM acetate was applied in WT (**C**) and *Slc26a6*$^{-/-}$ (**D**) ventricular myocytes. EIPA (5 μM) was added to inhibit the $Na^+/H^+$ exchanger during acetate application. **E**. Effects of 40 mM acetate on the CaT and sarcomere length in WT and *Slc26a6*$^{-/-}$ ventricular myocytes. EIPA (5 μM) was added to inhibit the $Na^+/H^+$ exchanger during acetate application. The recovery process after wash out of acetate for *Slc26a6*$^{-/-}$ myocytes is much slower than that of WT myocytes. The black traces showed the CaT, and the blue traces showed the sarcomere length.

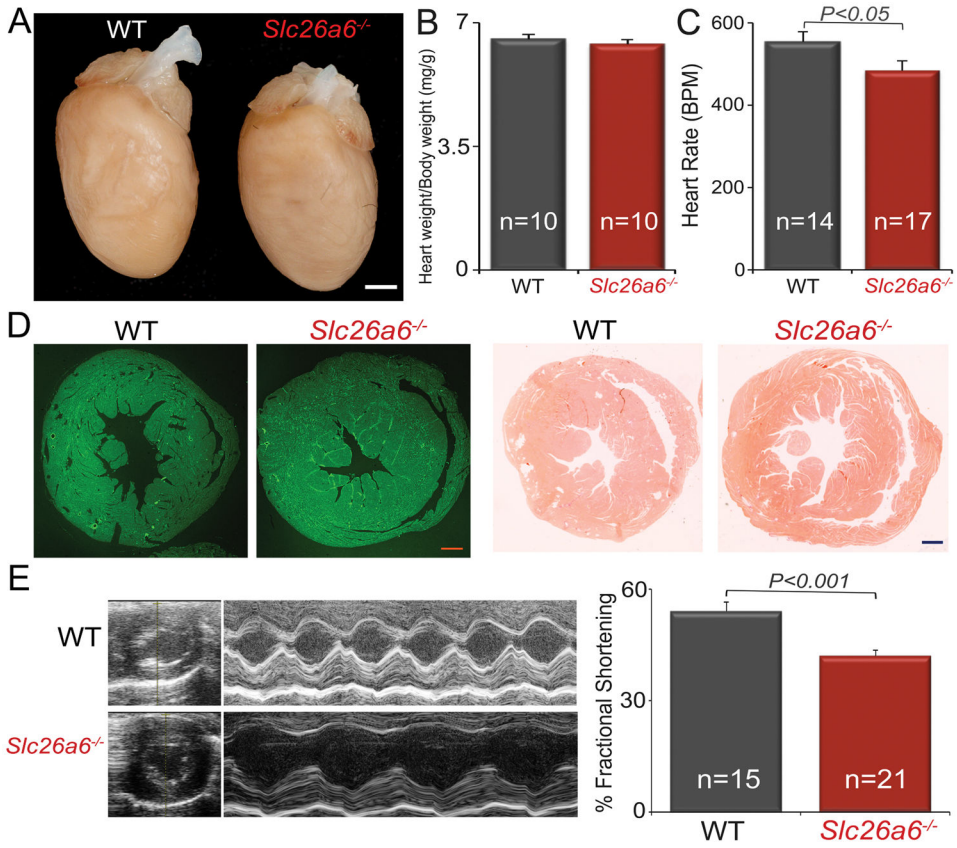


**Figure 4. *Slc26a6*$^{-/-}$ mice demonstrate worsening fractional shortening and sinus bradycardia**

**A.** Photomicrographs of whole heart of WT and *Slc26a6*$^{-/-}$ mice (Scale bar,1 mm). **B**. Summary for heart/body weight ratio in mg/g. **C**. Heart rate. (BPM: beat per minute). **D**. Wheat germ agglutinin (left two panels) and Picrosirius Red (right two panels) staining of cardiac sections from WT and *Slc26a6*$^{-/-}$ mice demonstrating no evidence of increase fibrosis in the knockout mice (scale bar, 0.5 mm). **E**. 2D and M-mode echocardiography from WT and *Slc26a6*$^{-/-}$ mice. The right panel shows summary data for fractional shortening (%FS), illustrating a significant decrease in %FS in KO mice compared to WT.

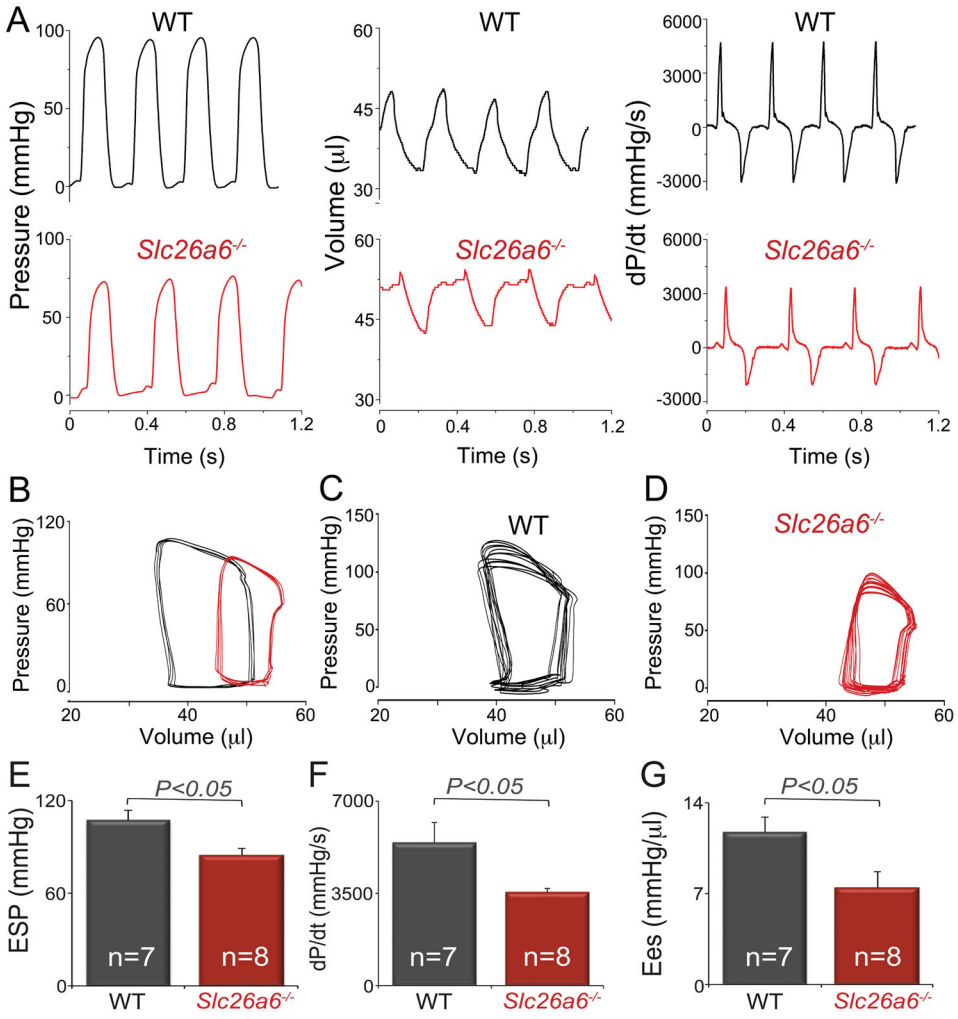


**Figure 5. Hemodynamics monitoring from *Slc26a6*$^{-/-}$ and WT mice demonstrates the reduced cardiac contractility in *Slc26a6*$^{-/-}$ mice**

**A**. Recording traces of left ventricular pressure, volume, and derivative of pressure with respect to time (dP/dt) from WT and *Slc26a6*$^{-/-}$ mice. **B**. P-V loop analysis. The pressure and volume have been calibrated. The volume calibration was performed using cuvette (P/N 910-1049, Millar Inc.) filled with fresh heparinized 37° C mouse blood. A series of P-V loops when the preload was altered in WT (**C**) and *Slc26a6*$^{-/-}$ mice (**D**). **E, F, G**. Summary data for end systolic pressure (ESP), maximum dP/dt, and the slope of the end systolic P-V relationship (Ees).

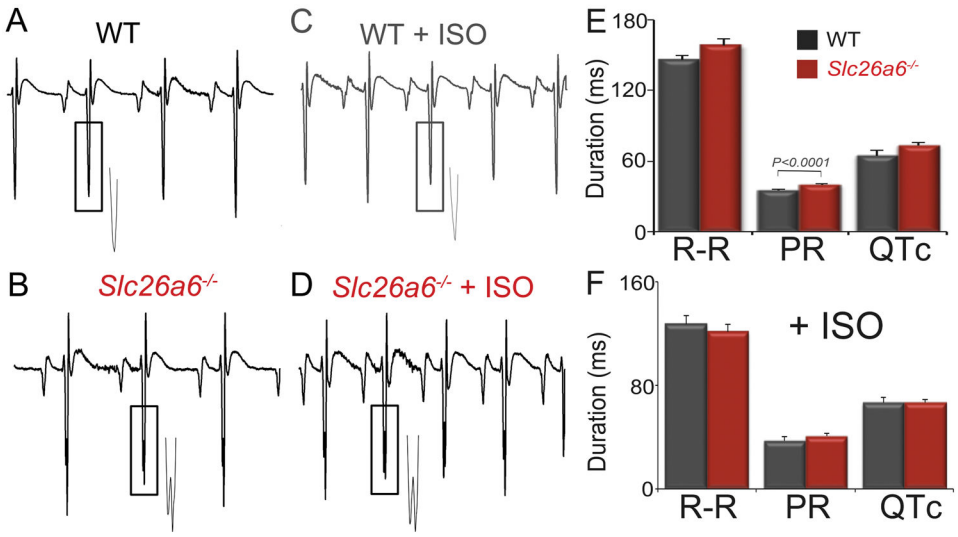


**Figure 6. ECG recordings from age-matched WT and *Slc26a6*$^{-/-}$ mice reveal evidence of fragmented QRS complexes in the knockout mice**

**A to D**. Representative ECG traces. The insets showed the enlarged traces marked by the rectangular boxes demonstrating fragmented QRS complexes observed only in *Slc26a6*$^{-/-}$ mice. **E.** ECG parameters in control condition and with isoproterenol (ISO) (**F**).

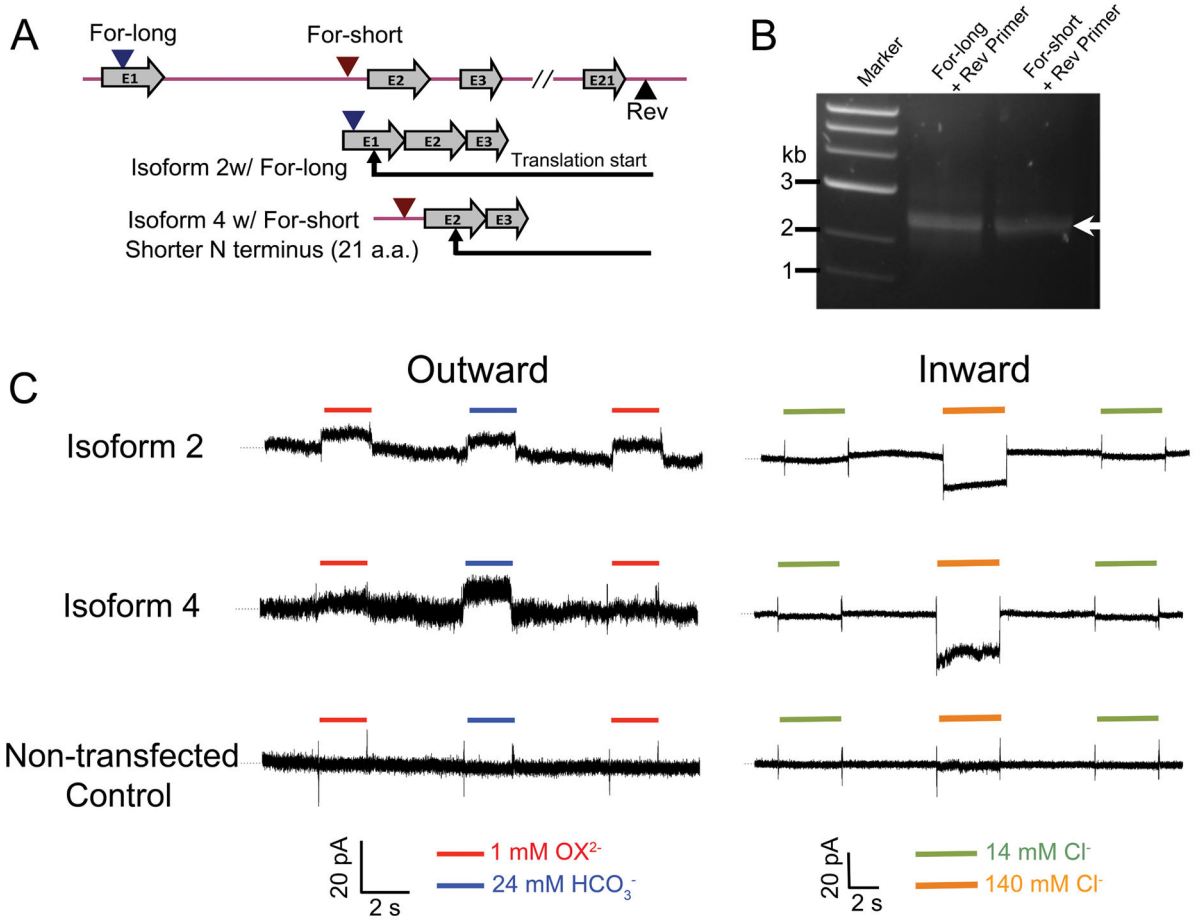


**Figure 7. Molecular identification and functional analysis of human cardiac SLC26A6 isoforms**

**A.** The cloning strategy. Two different forward primers, For-long and For-short, were designed, corresponding to the genomic DNA sequence in chromosome 3 (NC_000003.12), one on 5′-UTR of exon 1 and the other on the intron sequence between exon 1 and exon 2, to verify isoforms having distinct 5′-UTR and/or 5′-end of coding sequence. The exon structure of the cloned isoforms was shown below. **B.** RT–PCR amplification of the full-length cDNA of human cardiac SLC26A6 isoforms (indicated by an arrow) using two sets of primers. **C.** Patch-clamp recordings and fast solution exchange to activate two heterologously expressed human cardiac SLC26A6 isoforms that we have obtained. The outward current was activated by the solution exchange diagram shown in Fig.1B, and the inward current was activated by the solution exchange diagram shown in Fig.1G. Recordings on non-transfected CHO cells were shown at the bottom. Dotted lines represent zero current.